arXiv:1610.03445v1 [cond-mat.mtrl-sci] 11 Oct 2016

Magnetic gap opening in rhombohedral stacked multilayer graphene from first principles

Betül Pamuk,[1] Jacopo Baima,[1] Francesco Mauri,[2,3,*] and Matteo Calandra[1,†]

[1] *CNRS, UMR 7590 and Sorbonne Universités, UPMC Univ Paris 06, IMPMC - Institut de Minéralogie, de Physique des Matériaux, et de Cosmochimie, 4 place Jussieu, F-75005, Paris, France*

[2] *Dipartimento di Fisica, Università di Roma La Sapienza, Piazzale Aldo Moro 5, I-00185 Roma, Italy*

[3] *Graphene Labs, Fondazione Istituto Italiano di Tecnologia, Via Morego, I-16163 Genova, Italy*

(Dated: October 12, 2016)

We investigate the occurrence of magnetic and charge density wave instabilities in rhombohedral stacked multilayer (3 to 8 layers) graphene by first principles calculations including exact exchange. Neglecting spin-polarization, an extremely flat surface band centered at the special point **K** of the Brillouin zone occurs at the Fermi level. Spin polarization opens a gap in the surface state by stabilizing an antiferromagnetic state. The top and the bottom surface layers are weakly ferrimagnetic in-plane (net magnetization smaller than $10^{-3}\mu_B$), and are antiferromagnetic coupled to each other. This coupling is propagated by the out-of-plane antiferromagnetic coupling between the nearest neighbors. The gap is very small in spin polarized generalized gradient approximation, while it is proportional to the amount of exact exchange in hybrid functionals. For trilayer rhombohedral graphene it is 38.6 meV in PBE0, in agreement with the 42 meV gap found in experiments. We study the temperature and doping dependence of the magnetic gap. At electron doping of $n \sim 7 \times 10^{11}$ cm^{-2} the gap closes. Charge density wave instabilities with $\sqrt{3} \times \sqrt{3}$ periodicity do not occur.

In a solid, at low enough density, the Coulomb energy dominates the single particle energy and electronic instabilities such as magnetic phases or even Wigner crystallization become possible. A reduction of the single-particle energy, and a consequent enhancement of the electron-electron interaction, can be obtained by considering a metallic system with a very flat single-particle band-dispersion. This unfortunately does not happen in graphene where the high Fermi velocity prevents electronic instability. The situation is however different in weakly doped Bernal-stacked (AB) even-multilayer graphene (see Fig. 1), as the single-particle bands become massive. Indeed, a spontaneously gapped ground state is observed already in suspended bilayer [1, 2] and four-layer graphene (1.5 meV gap)[3].

Even more favorable to electronic instabilities is rhombohedral-stacked (ABC) multilayer graphene. Neglecting spin polarization, tight-binding and density functional theory (DFT) calculations find bulk rhombohedral graphite to be metallic with a high Fermi velocity (see grey region in Fig. 1). On the contrary, within these approximations, rhombohedral-stacked multilayer graphene (RSMG) displays the occurrence of an extremely flat surface state at the Fermi level (see Fig. 1) located at the **K** point of the graphene Brillouin zone (BZ) [4–9]. The extension of the surface state in the BZ increases with increasing thickness and saturates at ≈ 7 layers. Its bandwidth is at most 2 meV for flakes of less than 8 layers. The extremely reduced bandwidth makes RSMG one of the strongest correlated systems known nowadays and an ideal candidate for correlated states even in the absence of d orbitals.

On the experimental side, only recently it has been possible to synthesize RSMG. Ouerghi *et al.* [10] found 5 layer RSMG on top of a cubic SiC substrate to be metallic with a very high density of states at the Fermi level, in agreement with spinless DFT predictions. More recent work on suspended ABC trilayer [11] seems to suggest that a gap as large as 42 meV occurs at the Fermi level. However, transport measurements with singly gated devices, where the charge density and the potential difference cannot be controlled independently, the gap is much smaller [12]. The origin of this gap state has been suggested to be related to a magnetic state in which the external layers are antiferromagnetic coupled while the in-plane spin state is ferrimagnetic [11, 13]. Finally, it is worth to mention that it has been claimed that RSMG flakes composed of 17 layers can be isolated from kish graphite [14]. However it is still unknown if a gap opens in these samples.

In this work, by using density functional theory calculations with several hybrid functionals we investigate the occurrence of charge and magnetic instabilities in RSMG. Furthermore we discuss the effect of doping and temperature on the interaction induced gap.

DFT calculations are performed using the CRYSTAL code [15] with the triple-ζ-polarized Gaussian type basis sets for the C atoms [16]. The PBE0 [17] and other hybrid functionals with several degrees of exact exchange (see Supplemental Material (SM)) have been used for DFT calculations. The band flatness and the extreme localization of the low energy states around the special point **K** require an ultradense sampling with an electronic k mesh of $516 \times 516 \times 1$. We used real space integration tolerances of 7-7-7-15-30, and with an energy tolerance of 10^{-11} Ha for the total energy convergence. Fermi-Dirac

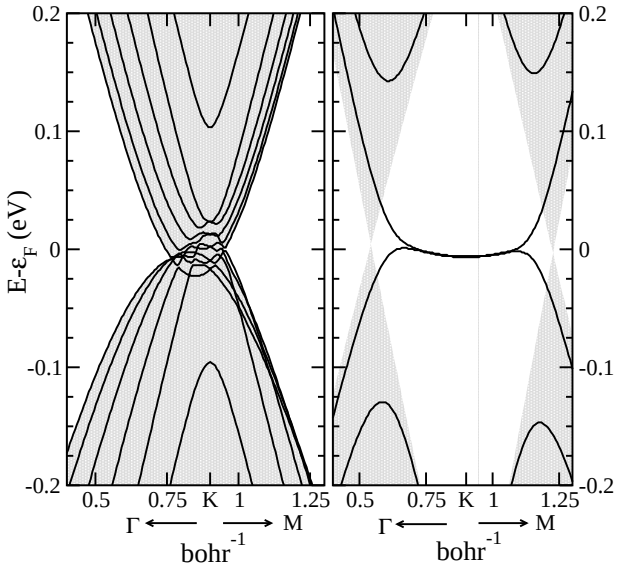

FIG. 1. Electronic structure (black lines) of a 10 layers Bernal (left) and Rhombohedral (right) stacked multilayer graphene calculated with the LDA functional. The grey regions are the bulk electronic structures projected over the surface.

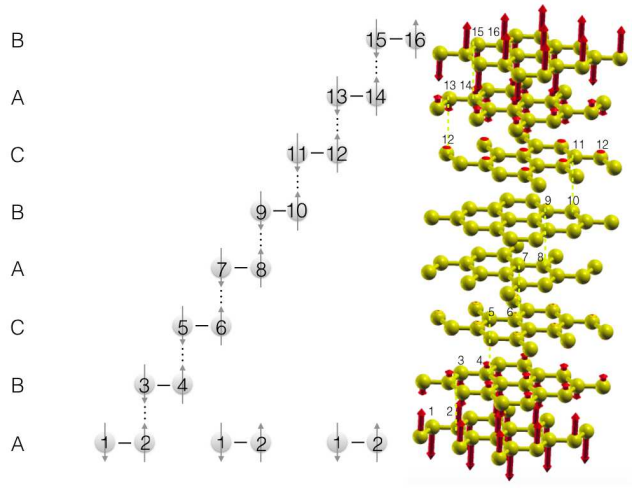

FIG. 2. Left: Schematic of the rhombohedral graphene with ABC stacking sequence. Solid lines represent the in-plane covalent bond, and the dashed lines represent the out-of-plane weak interlayer bond. The arrows represent only the direction of the spin, as the magnitude is layer dependent. Right: The atomic structure of rhombohedral 8-layer graphene.

smearing for the occupation of the electronic states is used for all of the calculations. The density of states is obtained with a Gaussian smearing of 0.00005 Ha. In the magnetic case, we fix the magnetic state in the first iteration of the self-consistent cycle and then we release the constraint. We choose an in-plane lattice parameter of $a = 2.461$ Å, and an inter-plane distance of 3.347 Å. A vacuum of 10.04 Å is placed between the periodic images along the z-direction.

We consider $N \geq 3$, N being the number of layers. We start the simulation from an initial magnetic state having ferromagnetic coupling in the surface layers and antiferromagnetic coupling between them. In both spin polarized PBE [18] and exact exchange functionals (HSE06, PBE0,..), we always converge to a magnetic state that is i) globally, an antiferromagnetic spin state, namely for each spin up band we have a spin down band degenerate in energy but localized on different atoms; ii) ferrimagnetic within the surface layers where the 2 atoms have opposite spins with slightly different magnetic moment; iii) with antiferromagnetic coupling between the top and bottom layers. The magnitude of the spin drops significantly further away from the surface. This magnetic state is similar to the one found in bilayer and trilayer graphene in the framework of Hubbard like models [11, 13] (the so-called layered antiferromagnetic state), however here the module of the magnetic moments in each outer surface layer are identical up to 0.001 μ_B, meaning that we are very close to an in-plane antiferromagnetic state than a ferrimagnetic state.

Fig. 2 shows a schematic diagram of rhombohedral graphene, with arrows representing the direction of the spin for all layers up to 8 layers. In rhombohedral graphene, total number of atoms is $N_{\rm atom} = N$, with each layer having 2 covalent bonded C atoms, only one of which is weakly bonded to the neighboring layer. The labeling of the atoms start from the bottom layer, where atom 1 is covalent bonded to atom 2, and atom 2 is weakly bonded to atom 3 of the next layer, and the labeling follows covalent to weak interlayer bond. The magnetic order we find is such that the odd numbered atoms have spin down, and the even numbered atoms have spin up, with the spin magnetic moments such that $\mu_i = -\mu_{\rm Natom-i+1}$. The outermost surface layers are ferrimagnetic with $\mu_1 > \mu_2$. In-plane and out-of-plane nearest neighbors are antiferromagnetic coupled.

Within spin polarized PBE, the local magnetic moments are essentially zero. The increase of the exact exchange component in the functional enhances the magnetic moments. The magnetic moments in the outermost layers are larger for 8-layer thick flakes and within PBE0 they are is as large as 10^{-2} bohr magnetons in magnitude (see table I). The magnetic moments for other functionals are shown in the supplemental material.

The PBE0 magnetic electronic structure for $3 \leq N \leq 8$ is shown in Fig. 3. Each band is doubly degenerate with spin up and down states having the same energy. Therefore globally the system is in an antiferromagnetic state. This magnetic order results in a gapped state, with the gap at the **K** point increasing with N. The surface bands are quite flat with a small asymmetry between the $\mathbf{\Gamma} \rightarrow \mathbf{K}$ and $\mathbf{K} \rightarrow \mathbf{M}$ directions that increases with N. This behavior is easily understood as for $N \rightarrow \infty$ the

TABLE I. The magnitude of the spin of each atom in $10^{-3}\mu_B$ for rhombohedral N-layer graphene. The spins are reported up to $\mu_{\mathrm{Natom}/2}$, and the spins of the rest of the atoms, as well as the direction of the spin can be obtained by $\mu_i = -\mu_{\mathrm{Natom}-i+1}$. This direction can be matched to the Fig. 2.

N	$\mu_1 = -\mu_{\mathrm{N_{atom}}}$	μ_2	μ_3	μ_4	μ_5	μ_6	μ_7	μ_8
3	-5.28	4.60	-2.73					
4	-7.32	6.33	-3.22	3.11				
5	-8.56	7.38	-3.62	3.43	-2.60			
6	-9.19	7.90	-3.82	3.58	-2.34	2.29		
7	-9.75	8.40	-4.11	3.84	-2.38	2.30	-1.93	
8	-10.04	8.64	-4.23	3.94	-2.34	2.24	-1.69	1.66

surface projected bulk bands of rhombohedral graphite should be recovered (see Fig. 1). More insight on the gap opening at **K** is obtained by analyzing the projected electronic bands on the atoms of the surface layers. The surface states are dominated by the p_z orbitals of two C atoms. On each surface layer, only the atom having no out-of-plane neighboring atoms contributes to the surface bands (see SM).

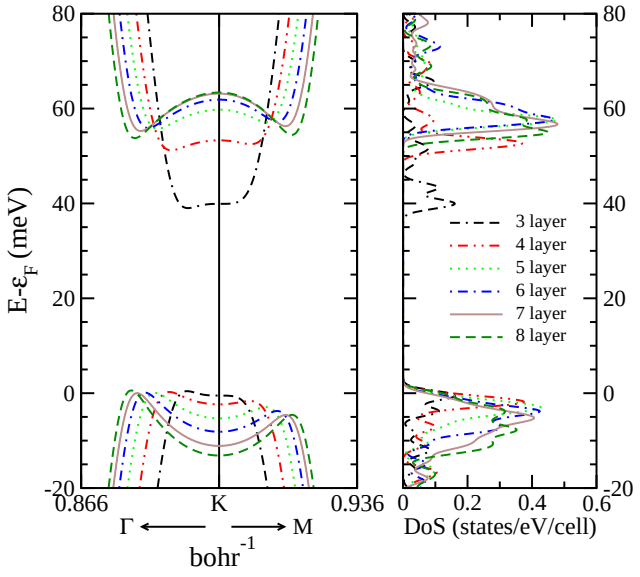

FIG. 3. The electronic band structure (left) and density of states (right) of the surface states of the magnetic state of the rhombohedral graphene up to 8 layers calculated with the PBE0 functional. The electronic bands are plotted around 0.035 bohr^{-1} of the **K** point along the path $\mathbf{\Gamma} \rightarrow \mathbf{K} \rightarrow \mathbf{M}$ and each band is spin degenerate.

We find the band gap for rhombohedral trilayer graphene to be $E_g = 38.6$ meV with the PBE0 functional. This result is in good agreement with the experimentally reported value of $E_g = 42$ meV in Ref. [11]. By using other functionals with different percentages of exact exchange and range separation we find smaller gaps as shown in the supplemental material. As the PBE0 gap gives the best agreement with experiment we use this functional for the rest of the paper.

The change in the band gap at zero temperature for different layers is shown in Fig. 3,4 and Table II. The band gap increases significantly from 3 to 4 layers, but saturates after 5 layers. At 8 layers, the gap starts to close slowly, with increasing deviation from the flat bands, in order to reach the bulk limit [19] shown in Fig. 1.

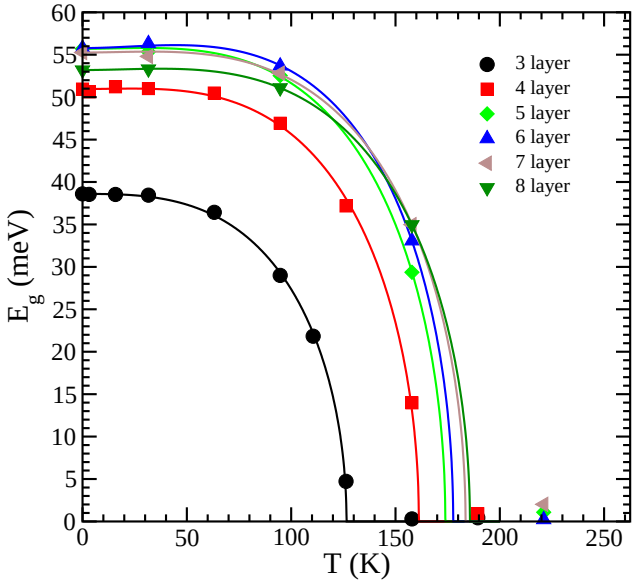

FIG. 4. Temperature dependence of the band gap, E_g, up to 8 layers. The dots are the data obtained with PBE0 functional. The lines are the result of the fit to the eq. (1).

As the gap is strongly temperature dependent in experiments and closes at $T_c = 34$ K[11], we study the antiferromagnetic gap as a function of temperature. This is done by including a Fermi-Dirac occupation of the electronic states. The temperature dependence of the gap is shown in Fig. 4. To obtain T_c, we fit the band gap to the function,

$$E_g(T) = E_g(0)\left[A\left(1-\frac{T}{T_c}\right)+(3-2A)\left(1-\frac{T}{T_c}\right)^2 +(A-2)\left(1-\frac{T}{T_c}\right)^3\right]^{1/2} \quad (1)$$

with the constants arranged such that the first and the second derivative of the curve is zero at the zero temperature limit. The temperature dependence of the band gap has a similar behavior to that obtained from the experiments in Ref. [11]. However, the thermal suppression of the gap is slower in our calculations, resulting in a larger $T_c = 126.5$ K, as compared to the experimental value of $T_c = 34$ K for trilayer graphene. We attribute the discrepancy between theory and experiments to the imperfect treatment of screening at the hybrid functional level.

Similar to what happens for the layer dependence of the band gap with the number of layers, T_c increases up to 5 layers, and then saturates and changes slowly. The T_c values and the fit parameter A of each layer are also shown in Table II for different number of layers.

TABLE II. The T_c values and the fit parameter A of eq. (1) of each layer.

N	$E_g(0)$ (meV)	T_c (K)	A
3	38.60	126.53	2.97
4	50.96	161.21	3.28
5	55.70	173.90	3.36
6	55.78	177.67	3.60
7	55.26	183.58	3.36
8	53.19	185.67	3.43

Contrary to the case of suspended samples, supported RSMG show a metallic behaviour [10]. A possible reason for this could be the presence of a substrate doping [11]. In order to verify this hypothesis, we consider n-doping of rhombohedral trilayer graphene. We use a compensating jellium background to enforce charge neutrality.

To estimate the number of electrons needed to close the gap, we have integrated the first peak of the density of states in Fig. 3. For the trilayer rhombohedral graphene an electron density of $n = 8.01 \times 10^{11}$ cm^{-2} (corresponding to $x = 0.00042$ electrons/cell) is needed to fill the flat conduction band region. This electron density increases to $n = 67.70 \times 10^{11}$ cm^{-2} for 8 layers. The results for the rest of the layers are presented in the SM.

We find that doping reduces the band gap. In agreement with our estimation from the density of states, the gap ultimately closes at $n \sim 7 \times 10^{11}$ cm^{-2}, to be compared to $n \sim 3 \times 10^{11}$ cm^{-2} found in experiments[11]. The combined effect of doping and temperature is shown in Fig. 5 (and in the SM). We conclude that substrate doping can be responsible of the differences between supported and suspended samples. We can also speculate that the critical doping to close the gap could grow by an order of magnitude by increasing the number of ABC stacked layers.

Up to now we consider the possibility of magnetic gap opening in RSMG. However, charge density wave instabilities could also open a gap via phonon softening. In order to validate this hypothesis, we calculate phonon

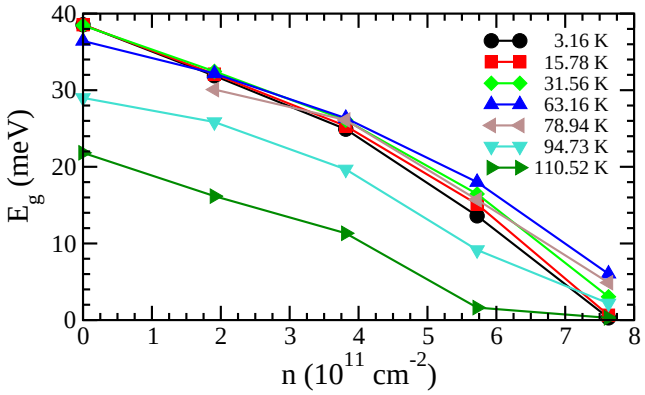

FIG. 5. Doping dependence of the band gap of rhombohedral trilayer graphene at different temperatures. The lines are to guide the eye.

frequencies at **Γ** and **K** by using the finite differences method and the spinless PBE0 functional in rhombohedral stacked trilayer graphene. We find that the largest softening occurs at the **K** point of the Brillouin zone [20] for the in-plane phonon mode. Despite PBE0 substantially softens the phonon frequencies with respect to PBE, all the phonon modes are stable so that a structural distortion compatible with a $\sqrt{3} \times \sqrt{3}$ periodicity is excluded. The magnitude of the phonon modes are also reported in the SM. Magnetism is then the most likely instability in RSMG.

In this Letter, we have analyzed the magnetic and charge instabilities in rhombohedral stacked multilayer graphene using spin-polarized hybrid functionals. While in the absence of spin-polarization an extremely flat surface state occurs at the Fermi level, the introduction of spin polarization leads to magnetic instabilities and opening of a gap in the surface state. The state is such that the surface layers are weakly ferrimagnetic in-plane, and the top and the bottom layers are antiferromagnetic coupled, which is propagated by the out-of-plane antiferromagnetic coupling between the nearest neighboring atoms. The globally stable state is antiferromagnetic where the spin up and spin down bands are degenerate. Within PBE0 the gap is found to agree with experiments on ABC trilayer graphene. We have shown that doping suppress the gap, explaining the experimental finding that a gap occurs in trilayer ABC graphene only in suspended samples. Finally, we study the possible occurrence of charge density wave instabilities with $\sqrt{3} \times \sqrt{3}$ supercell. We found that no charge density wave occurs so that the gap opening seen in experiments is only due to the magnetic coupling of the surface atoms in the multilayers. Our work demonstrate that the inclusion of exact exchange in first principles calculations and an ultradense sampling of the Brillouin zone are crucial in order to explain the magnetic and structural instabilities of rhombohedral-stacked multilayer graphene.

This work is supported by the Graphene Flagship and by Agence Nationale de la Recherche under the reference no ANR-13-IS10-0003-01.

* francesco.mauri@uniroma1.it
† matteo.calandra@impmc.upmc.fr

[1] F. Freitag, J. Trbovic, M. Weiss, and C. Schönenberger, Phys. Rev. Lett. **108**, 076602 (2012).
[2] J. V. Jr, L. Jing, W. Bao, Y. Lee, P. Kratz, V. Aji, M. Bockrath, C. N. Lau, C. Varma, R. Stillwell, D. Smirnov, F. Zhang, J. Jung, and A. H. MacDonald, Nat. Nano. **7**, 156 (2012).
[3] A. L. Grushina, D.-K. Ki, M. Koshino, A. A. L. Nicolet, C. Faugeras, E. McCann, M. Potemski, and A. F. Morpurgo, Nat. Comm. **6**, 6419 (2015).
[4] M. Koshino, New Journal of Physics **15**, 015010 (2013).
[5] J. Jung and A. H. MacDonald, Phys. Rev. B **88**, 075408 (2013).
[6] S. Latil and L. Henrard, Phys. Rev. Lett. **97**, 036803 (2006).
[7] R. Xiao, F. Tasnádi, K. Koepernik, J. W. F. Venderbos, M. Richter, and M. Taut, Phys. Rev. B **84**, 165404 (2011).
[8] B.-R. Wu, Applied Physics Letters **98**, 263107 (2011).
[9] M. Otani, M. Koshino, Y. Takagi, and S. Okada, Phys. Rev. B **81**, 161403 (2010).
[10] D. Pierucci, H. Sediri, M. Hajlaoui, J.-C. Girard, T. Brumme, M. Calandra, E. Velez-Fort, G. Patriarche, M. G. Silly, G. Ferro, V. Soulire, M. Marangolo, F. Sirotti, F. Mauri, and A. Ouerghi, ACS Nano **9**, 5432 (2015), pMID: 25893537, http://dx.doi.org/10.1021/acsnano.5b01239.
[11] Y. Lee, D. Tran, K. Myhro, J. Velasco, N. Gillgren, C. Lau, Y. Barlas, J. Poumirol, D. Smirnov, and F. Guinea, Nat. Comm. **5**, 5656 (2014).
[12] W. Bao, L. Jing, J. V. Jr, Y. Lee, G. Liu, D. Tran, B. Standley, M. Aykol, S. B. Cronin, D. Smirnov, M. Koshino, E. McCann, M. Bockrath, and C. N. Lau, Nat. Phys. **7**, 948 (2011).
[13] R. E. Throckmorton and O. Vafek, Phys. Rev. B **86**, 115447 (2012).
[14] Y. Henni, H. P. O. Collado, K. Nogajewski, M. R. Molas, G. Usaj, C. A. Balseiro, M. Orlita, M. Potemski, and C. Faugeras, Nano Letters **16**, 3710 (2016), pMID: 27164265, http://dx.doi.org/10.1021/acs.nanolett.6b01041.
[15] R. Dovesi, R. Orlando, A. Erba, C. M. Zicovich-Wilson, B. Civalleri, S. Casassa, L. Maschio, M. Ferrabone, M. D. L. Pierre, P. D'Arco, Y. Noël, M. Causà, M. Rérat, and B. Kirtman, Int. J. Quantum Chem. **114**, 1287 (2014).
[16] M. F. Peintinger, D. V. Oliveira, and T. Bredow, Journal of Computational Chemistry **34**, 451 (2013).
[17] C. Adamo and V. Barone, J. Chem. Phys. **110**, 6158 (1999).
[18] J. P. Perdew, K. Burke, and M. Ernzerhof, Phys. Rev. Lett. **77**, 3865 (1996).
[19] C.-H. Ho, C.-P. Chang, and M.-F. Lin, Phys. Rev. B **93**, 075437 (2016).
[20] M. Lazzeri, C. Attaccalite, L. Wirtz, and F. Mauri, Phys. Rev. B **78**, 081406 (2008).